# Acid ceramidase controls proteasome inhibitor resistance and is a novel therapeutic target for the treatment of relapsed/refractory multiple myeloma

Ryan T. Bishop,[1] Tao Li,[1] Praneeth R. Sudalagunta,[2] Mostafa M. Nasr,[1,3] Karl J. Nyman,[1,3] Raghunandan R. Alugubelli,[4] Mark B. Meads,[1,5] Jeremy S. Frieling,[1] Niveditha Nerlakanti,[1,3] Marilena Tauro,[1] Bin Fang,[6] Steven Grant,[7] John M. Koomen,[6,8] Ariosto S. Silva,[2] Kenneth H. Shain[1,5] and Conor C. Lynch[1]

[1]Department of Tumor Metastasis and Microenvironment, H. Lee Moffitt Cancer Center and Research Institute, Tampa, FL; [2]Department of Metabolism and Physiology, H. Lee Moffitt Cancer Center and Research Institute, Tampa, FL; [3]Cancer Biology Ph.D. Program, University of South Florida, Tampa, FL; [4]Collaborative Data Services Core, H. Lee Moffitt Cancer Center and Research Institute, Tampa, FL; [5]Department of Malignant Hematology, H. Lee Moffitt Cancer Center and Research Institute, Tampa, FL; [6]Molecular Medicine, H. Lee Moffitt Cancer Center and Research Institute, Tampa, FL; [7]Virginia Commonwealth University (VCU) Massey Cancer Center Richmond, VA and [8]Department of Molecular Oncology, H. Lee Moffitt Cancer Center and Research Institute, Tampa, FL, USA

**Correspondence:** C.C. Lynch
conor.lynch@moffitt.org

**Received:** April 23, 2024.
**Accepted:** November 27, 2024.
**Early view:** December 5, 2024.

**https://doi.org/10.3324/haematol.2024.285587**

## Supplementary Materials and Methods:

### Sample Preparation and RNA Sequencing Analysis: PMRC Cohort

Fresh BM aspirate cells were enriched for CD138 expression using Miltenyi (Bergisch Gladbach, Germany) 130-051-301 antibody-conjugated magnetic beads. 1.0 x $10^6$ viably frozen CD138+ cells were shipped for molecular analysis in the context of the ORIEN Avatar program.

*Nucleic Acid Extraction:* For frozen tissue DNA extraction, Qiagen QIASymphony DNA purification was performed, generating 213 bp average insert size. For frozen tissue RNA extraction, Qiagen RNAeasy plus mini kit was performed, generating 216 bp average insert size.

*RNA Sequencing* was performed using the Illumina TruSeq RNA Exome with single library hybridization, cDNA synthesis, library preparation, sequencing (at either 100 or 150 bp paired reads) to a coverage of 100M total reads / 50M paired reads.

RNA-seq Tumor Pipeline Analysis is processed according to the workflow outlined below using GRCh38/hg38 human genome reference sequencing and GenCode build version 32.

*Adapter trimming:* Adapter sequences are trimmed from the raw tumor sequencing FASTQ file. Adapter-trimming via *k*-mer matching is performed along with quality-trimming and filtering, contaminant-filtering, sequence masking, GC-filtering, length filtering and entropy-filtering. The trimmed FASTQ file is used as input to the read alignment process.

*Read Alignment:* The tumor adapter-trimmed FASTQ file is aligned to the human genome reference (GRCh38/hg38) and the Gencode genome annotation v32 using the STAR aligner. The STAR aligner generates multiple output files used for Gene Fusion Prediction and Gene Expression Analysis.

*RNA expression:* RNA expression values are calculated and reported using estimated mapped reads, Fragments Per Kilobase of transcript per Million mapped reads (FPKM), and Transcripts Per Million mapped reads (TPM) at both transcript level and gene level based on transcriptome alignment generated by STAR. Gene expression data was obtained from DNAnexus files containing FPKM and TPM values for 59,368 records. Among these, 19,933 were protein coding genes, which were further analyzed; the remainder were discarded. For each gene/sample, we have calculated $\log2(FPKM+10^{-3})$ and removed any genes whose values for quartile 1 and quartile 3 were the same (i.e., any gene must be expressed in at least 25% of samples to be considered in this analysis). The remaining 16,738 genes were Z-normalized across all samples using MATLAB's function *normalize*.

### Cell lines, culture conditions and compounds

## Supplementary Figures and Legends

Luciferase-labeled MM cells, 5TGM1-Luc (RRID: CVCL_VI66) and U266-Luc (RRID: CVCL_0566) were obtained from University of Texas, Health Science Center at San Antonio, TX (2012) and University of Virginia, VA (2014), respectively. MM1.S were obtained in 2015 from ATCC (RRID: CVCL_8792) and OPM2 was obtained in 2015 from Dr. Kenneth Shain (Moffitt Cancer Center; RRID: CVCL_1625). Isogenic PI-sensitive and resistant pairs U266 and PSR[1], RPMI8226 (RRID: CVCL_0014) and B25 [2], were obtained from Dr. Steven Grant (VCU-Massey) and ANBL-6 (RRID:CVCL_5425) and V10-R[3] pairs were obtained from Dr. Kenneth Shain (Moffitt Cancer Center). C300R, C100R and C40R (PI-resistant 5TGM1-Luc) cells were generated in house by continued culture in increasing concentration of carfilzomib for 3 months. C300R, C100R and C40R were exposed to 300nM, 100nM or 40nM maximum doses of carfilzomib, respectively. PI-resistant cell lines were maintained through bi-weekly 24-hour dosing with either bortezomib (30nM) or carfilzomib (300nM), cells were not used for five days following PI-treatment. All MM cell lines were maintained below $1x10^6$ cells/ml in RPMI-1640 containing 10% heat-inactivated FBS (PEAK, PK-FBS1), 1% penicillin and streptomycin and used within 20 passages. ANBL-6 and V10-R are IL-6 dependent cell lines, as such 1ng/ml IL-6 (R&D systems, HZ-1019) was added in cultures and all subsequent experiments. Human MSCs were obtained from Lonza (PT-2501) and cultured in αMEM (Gibco # 12561056) with 10% heat-inactivated qualified FBS (Gibco #26140079). Cells have recently tested negative for mycoplasma by PCR in December 2022 (Bulldog Bio, Cat #: 25233), and were additionally authenticated against ATCC, DSMZ or ExPASy STR profiles. The acid ceramidase inhibitors ceranib-2 (#11092), LCL-521 (#29738), carmofur (#14243) and ARN-14988 (#24284) and the proteasome inhibitors, bortezomib (#10008822) and carfilzomib (#17554) were purchased from Selleckchem. The acid ceramidase activity probe RBM14C12 (#860855), C6 ceramide (d18:1/6:0, # 860506) Huzzah-S1-P (#360492) and Huzzah-HSA (#360000) were purchased from Avanti polar lipids.

**Lentiviral Transductions**

Lentiviral particles with 4 individual shRNAs were generated following transformation of HEK-293 cells. MM cells were transduced with either ASAH1-targeting shRNA or non-targeting shRNA control lentivirus by spinfection with vectofusin-1 (Miltenyi Biotec # 130-111-163) at an MOI of 5. Cells were selected with puromycin (2μg/ml) for 72 hours. Knockdown was confirmed by immunoblotting. PSR-RFP were generated as above using lentiviral particles (Qiagen CLS-PCR-8) and FACS sorted.

**Acid ceramidase activity assay**

## Supplementary Figures and Legends

To determine ceramidase activity in intact cells ($5\times10^4$ cells/well) were seeded in 96-well plates in 100µl medium or PBS containing 40 µM RBM14C12 fluorogenic substrate incubated for 24 h at 37°C in a 5% CO2 atmosphere. To examine the effect of ceramidase inhibitors, cells were incubated with RBM14C12 for 3 hours. The reaction was stopped by addition of methanol followed by NaIO4 (2.5 mg/ml in 200 mM glycine/NaOH buffer, pH 10.6). After 1 h at 37°C, 100µl of 200 mM glycine/NaOH buffer were added, and fluorescence detected at 355/460nm excitation/emission wavelengths on a SpectraMax Microplate Reader (Molecular Devices, Sunnyvale, CA).

**Immunoblotting**

MM cells were lysed in RIPA buffer (150 mM NaCl, 1 mM EDTA, 1% Triton X-100, 1% sodium deoxycholate, 0.1% SDS, 20 mM Tris, pH 8). Protein concentration was determined by BCA (Pierce, Waltham, MA, USA; #23225). Blots were blocked in 5% BSA or TBS-T for 1 h followed by incubation with primary antibody overnight at 4°C. Primary antibodies were anti-ASAH1 (Thermofisher #HPA005468 or Pro-sci Inc #4741) , anti-actin (CST #3700), anti-BCL2 (CST #4223), anti-pBCL S70 (CST #2827), anti-MCL-1 (CST #94296), anti-p-MCL1 Thr163 (CST #14765), anti-vinculin (CST #13901) and diluted in blocking buffer. Blots were washed in TBS-T and incubated with either anti-rabbit IgG or anti-mouse IgG HRP-conjugated secondary antibodies (CST#7074 and #7076) and developed by enhanced chemiluminescence and imaging by LI-COR Odyssey Fc.

**Viability and dose response assays**

MM cell lines were plated in 96-well plates at a density of 2×105 cells/ml. Cells were treated with vehicle or indicated compounds. Cell viability was assessed at 24 or 72 hours by the MTT assay following the manufacturer's instructions (CellTiter 96, #G3582, Pierce.) The absorbance was measured at 490nm after 3 hours of incubation at 37°C. IC50s were calculated in Prism (version 9.3.1). Synergy matrices were calculated and generated using Combenefit.

***Ex vivo* drug sensitivity characterization: PMRC cohort**. An *ex vivo* assay was used to quantify the chemosensitivity of primary MM cells. Fresh BM aspirate cells were enriched for $CD138^+$ expression using Miltenyi (Bergisch Gladbach, Germany) 130-051-301 antibody-conjugated magnetic beads. MM cells ($CD138^+$) were seeded in Corning (Corning, NY) CellBIND 384 well plates with collagen I and previously established human-derived stroma, containing approximately 4000 MM cells and 1000 stromal cells. Each well was filled with 80 µL of Roswell

## Supplementary Figures and Legends

Park Memorial Institute (RPMI) 1640 media supplemented with fetal bovine serum (FBS, heat inactivated), penicillin/streptomycin, and patient-derived plasma (10%, freshly obtained from patient's own aspirate, filtered) and left overnight for adhesion of stroma. The next day, drugs were added using a robotic plate handler so that every drug/combination was tested at 5 (fixed concentration ratio, for combinations) concentrations (1:3 serial dilution) in two replicates. Negative controls (supplemented growth media with and without the vehicle control dimethyl sulfoxide (DMSO)) were included, as well as positive controls for each drug (cell line MM1.S at highest drug concentration). Plates were placed in a motorized stage microscope (EVOS Auto FL, Life Technologies, Carlsbad, CA) equipped with an incubator and maintained at 5% $CO_2$ and 37 °C. Each well was imaged every 30 min for a total duration of up to 6 days. A digital image analysis algorithm[4] was implemented to determine changes in viability of each well longitudinally across the 96 or 144 hr intervals. This algorithm computes differences in sequential images and identifies live cells with continuous membrane deformations resulting from their interaction with the surrounding extracellular matrix. These interactions cease upon cell death. By applying this operation to all 288 images acquired for each well, we quantified non-destructively, and without the need to separate the stroma and MM, the effect of drugs as a function of concentration and exposure time. Digital image analysis computes percent viability of MM cells for each time point and experimental condition (drug and concentration). For each patient-drug, we have a dose-time-response surface, which is abstracted into AUC (area under the curve), which is an area/integral measure of *ex vivo* response to therapy computed by taking an average of all *ex vivo* responses across all time (first 96h) and concentration.

**Flow cytometry**

For *ex vivo* analysis, tibia and femur were used to assess tumor burden by RFP or HLA-A/B/C expression. Tibial ends were excised, whole bone marrow was isolated by centrifugation at 10,000g for 10 seconds. Red blood cells were lysed by RBC lysis buffer (R7757, Sigma-Aldrich) as per manufacturers guidelines. Bone marrow cells were subject to viability staining with Zombie Near-Infrared (NIR; 1:500; 423105, BioLegend). Appropriate compensation and fluorescence-minus-one (FMO) controls were generated in parallel either with aliquots of bone marrow cells or PSR RFP+/-. Stained controls and samples were analyzed using BD Biosciences LSRII flow cytometer. The percentage of RFP+ or HLA-expressing cells was gated on singlet live bone marrow cells. The presence of BCL-2 and MCL-1 was assessed in HLA-expressing cells. FCS Express 7 was used to perform gating post acquisition.

## Supplementary Figures and Legends

**Microcomputed Tomography.**

Harvested tibiae were fixed in 4% PFA for 48 hours. Tibiae from mice from all time points were centralized and were subjected to micro-computed topography (μCT) scanning using Scanco μ35 scanner to elucidate bone volume data at the proximal tibial metaphases. Individual bone scans were deidentified using numerical codes during, and reidentified post analyses in a blinded fashion. Evaluation of trabecular bone microarchitecture was performed in a region that consisting of 1000 μm, beginning 120 μm from the growth plate. A three-dimensional cubical voxel model of bone was built and calculations were made for relative bone volume per total volume (BV/TV), trabecular number (Tb.N), trabecular thickness (Tb.Th), trabecular spacing (Tb.Sp) and connectivity density (Conn.D).

**Phosphoproteomics**

PI-resistant PSR or B25 cells that were transduced with control or ASAH1-targeting shRNA (ASAH1 KD) were subject to phosphoproteomic analysis. Cells were lysed in denaturing buffer containing 8 M urea, 20 mM HEPES (pH 8), 1 mM sodium orthovanadate, 2.5 mM sodium pyrophosphate and 1 mM β-glycerophosphate. Bradford assays determined the protein concentration for each sample. Aliquots of 200 μg were prepared for global phosphorylation. Protein disulfides were reduced with 4.5 mM DTT at 60 °C for 30 minutes and then cysteines were alkylated with 10 mM iodoacetamide for 20 minutes in the dark at room temperature. Trypsin digestion was carried out at room temperature overnight with enzyme to substrate ratio of 1:20, and tryptic peptides were acidified with aqueous 1% trifluoroacetic acid (TFA) and desalted with C18 Sep-Pak cartridges according to the manufacturer's procedure. For global phosphorylation, 200 μg of each tryptic digest was TMT labeled. Label incorporation was verified to be >95% by LC-MS/MS and spectral counting. The samples were then pooled and lyophilized. The TMT channel layouts were:

126C PSR control Rep1; 127N PSR KD Rep1; 127C PSR control Rep2; 128N PSR KD Rep2; 128C PSR control Rep3; 129N PSR KD Rep3; 129C PSR control Rep4; 130N PSR KD Rep4; 130C B25 control Rep1; 131N B25 KD Rep1; 131C B25 control Rep2; 132N B25 KD Rep2; B25 control Rep3; 133N B25 KD Rep3; 133C B25 control Rep4; 134N B25 KD Rep4.

After lyophilization, TMT-labeled peptides were redissolved in 200 μL of aqueous 20 mM Ammonium Formate, (pH 10.0). The high pH reversed phase liquid chromatography (bRPLC) separation was performed on a XBridge 4.6 mm x 100 mm column packed with BEH C18 resin,

## Supplementary Figures and Legends

3.5 µm particle size, 130 Å pore size (Waters). bRPLC Solvent A was aqueous 2% ACN with 5 mM Ammonium Formate, pH 10.0. Peptides were eluted by: 5% bRPLC B (aqueous 90% acetonitrile with 5 mM Ammonium Formate, pH 10.0) for 10 minutes, 5% - 15% B in 5 minutes, 15-40% B in 47 minutes, 40-100% B in 5 minutes and 100% B held for 10 minutes, followed by re-equilibration at 1% B. The flow rate was 0.6 ml/min, and 12 concatenated fractions were collected. Vacuum centrifugation (Speedvac, Thermo) dried the samples. TMT-labeled peptides were re-dissolved in immobilized metal affinity chromatography (IMAC) loading buffer containing aqueous 0.1% TFA and 85% acetonitrile. Phosphopeptides were enriched using IMAC resin (Cell Signaling Technology # 20432) on a Kingfisher (Thermo). IMAC resin was washed with loading buffer. Peptides were incubated with 10 µL of resin for 30 minutes at room temperature with gentle agitation. The IMAC resin was washed twice with loading buffer followed by wash buffer (aqueous 80% ACN, 0.1% TFA). Phosphopeptides were eluted with aqueous 50% ACN, 2.5% Ammonia. The volume was reduced to 20 µl via vacuum centrifugation.

A nanoflow ultra-high performance liquid chromatograph and nanoelectrospray orbitrap mass spectrometer (RSLCnano and Q Exactive HF-X, Thermo) were used for LC-MS/MS. The sample was loaded onto a pre-column (C18 PepMap100, 2 cm length x 100 µm ID packed with C18 reversed-phase resin, 5 µm particle size, 100 Å pore size) and washed for 8 minutes with aqueous 2% acetonitrile and 0.1% formic acid. Trapped peptides were eluted onto the analytical column, (C18 PepMap100, 25 cm length x 75 µm ID, 2 µm particle size, 100 Å pore size, Thermo). A 120-minute gradient was programmed as: 95% solvent A (aqueous 2% acetonitrile + 0.1% formic acid) for 8 minutes, solvent B (aqueous 90% acetonitrile + 0.1% formic acid) from 5% to 38.5% in 90 minutes, then solvent B from 50% to 90% B in 7 minutes and held at 90% for 5 minutes, followed by solvent B from 90% to 5% in 1 minute and re-equilibration for 10 minutes using a flow rate of 300 nl/min. Spray voltage was 1900 V. Capillary temperature was 275 °C. S lens RF level was set at 40. Top 20 tandem mass spectra were collected in a data-dependent manner. The resolution for MS and MS/MS were set at 60,000 and 45,000 respectively. Dynamic exclusion was 15 seconds for previously sampled peaks.

MaxQuant[5] (version 1.6.14.0) was used to identify peptides using the UniProt human database (March 2020) and quantify the TMT reporter ion intensities. Up to 2 missed trypsin cleavages were allowed. The mass tolerance was 20 ppm first search and 4.5 ppm main search. Reporter ion mass tolerance was set to 0.003 Da. Minimal Precursor intensity fraction 0.75. Carbamidomethyl cysteine was set as fixed modification. Phosphorylation on Serine/Threonine/Tyrosine and Methionine oxidation were set as variable modifications. Both peptide spectral match (PSM) and protein false discovery rate (FDR) were set at 0.05. Match

## Supplementary Figures and Legends

between runs feature was activated to carry identifications across samples. For data upload to PRIDE/ProteomeXchange, similar database searches were performed with Mascot (www.matrixscience.com) in Proteome Discoverer (Thermo). Perseus[6] (version 2.0.3.1) was used to perform quality control, log2 transformations, imputation, median subtraction and z-score normalization, annotation, and statistical analyses. T-tests were performed with a permutation-based false discovery rate (FDR <0.01). Kinase and phosphatase activity inference was calculated using the ROKAI explorer[7].

**Statistical analysis**

Quantified data are represented as mean with SD when applicable. For statistical analyses of any two treatment groups, Student t test was applied. For statistical analyses of three groups or more, one-way ANOVA with Bonferroni correction was performed in Prism version 9. Differences were considered significant if P < 0.05 (*). Increasing levels of significance are denoted by asterisks (** P<0.01, *** P<0.001 **** P<0.0001 or n.s., not significant).

Supp Figure 1

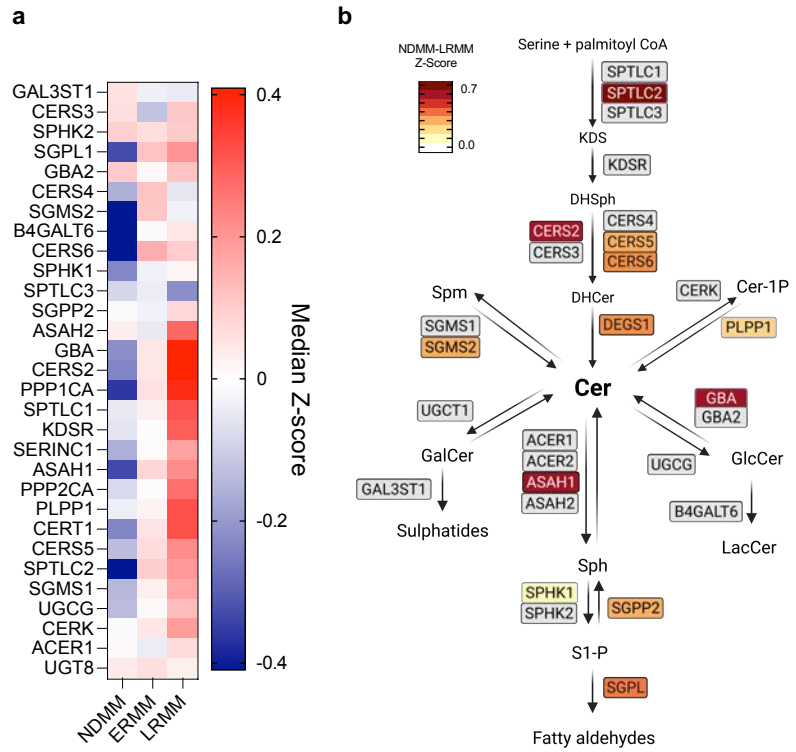


## Supplementary Figures and Legends

**Supplementary Figure 1. Sphingolipid metabolism is elevated in relapsed/refractory multiple myeloma.**

**a.** showing median mRNA z-score for 30 sphingolipid genes in newly diagnosed (NDMM; n=187), early relapse multiple myeloma (ERMM; n=303) and late relapse multiple myeloma (LRMM, n=182) patients.

**b.** Diagram of genes involved in the metabolism of sphingolipids. Genes with no significant differences in expression shown in gray boxes. Genes that were significantly enriched in both ERMM and LRMM patients compared to NDMM are colored. Colors represent difference between NDMM and LRMM median z-scores for each gene (LRMM-NDMM) as shown by the color bar in the upper left of the panel.

**Supplementary Figures and Legends**

Supp Figure 2

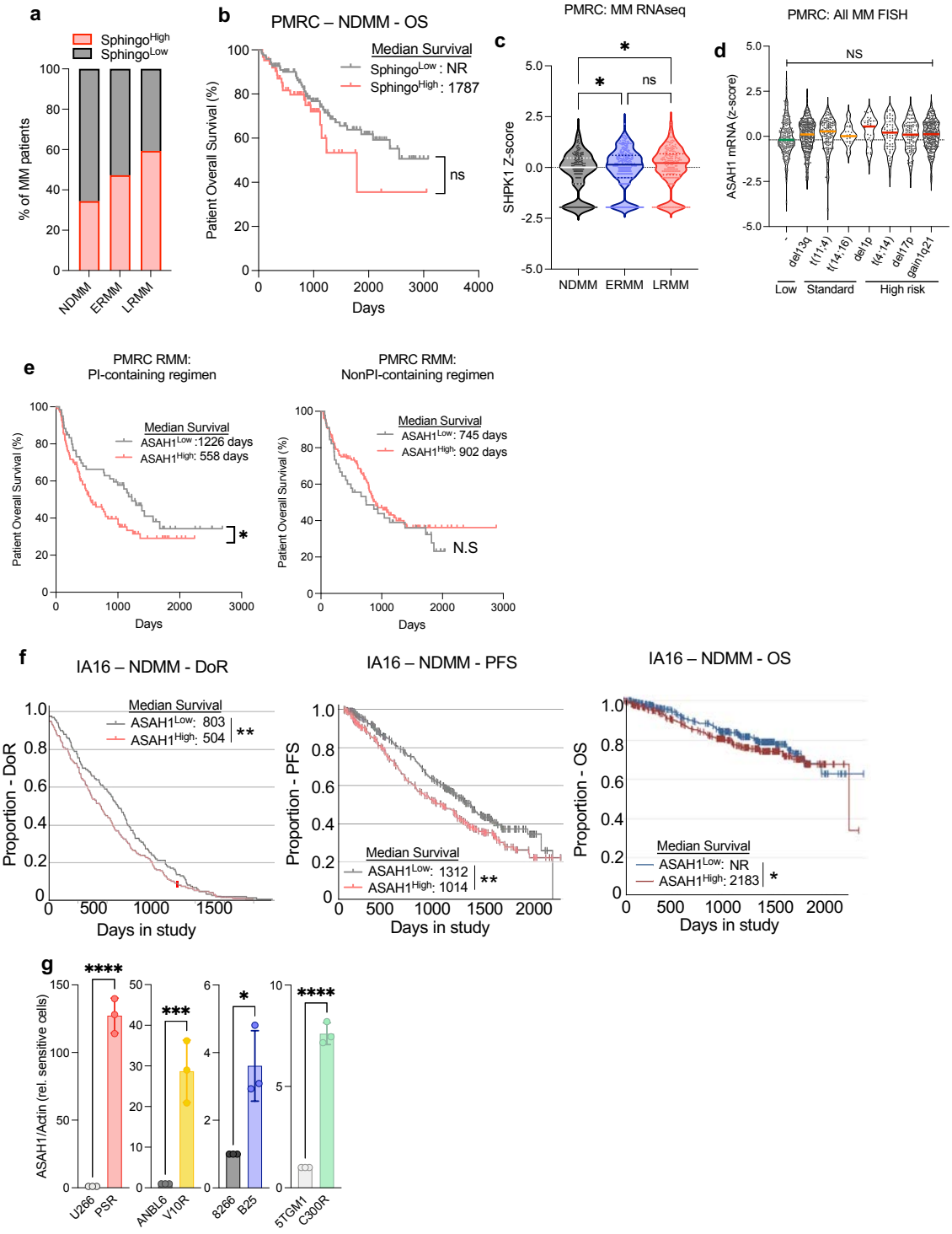


## Supplementary Figures and Legends

**Supplementary Figure 2. ASAH1 is elevated in relapsed/refractory multiple myeloma and correlates with reduced survival times**

**a.** Percentage of patients in Sphingo$^{Low}$ and Sphingo$^{High}$ clusters in NDMM (n=187), ERMM (n=303) and LRMM (n=182).

**b.** Kaplan-Meier plot of overall survival NDMM patients in Sphingo$^{Low}$ (n=113) and Sphingo$^{High}$ (n=74) clusters. Inset indicates median survival in days. NR = median survival not reached.

**c.** Violin plot showing expression of SPHK1 in NDMM (n=187), ERMM (n=303) and LRMM (n=182). Dots represent individual patients.

**d.** Violin plots showing expression of ASAH1 in all MM patients with no risk factors (-, n= 231) or t(11;4) (n=144), t(14;16) (n=23), t(4;14) (n=64), del1p (n=30) , del13q (n=311), del17p (n=113), gain1q21 (n=293) cytogenetic risk factors.

**e.** Kaplan-Meier plots of overall survival of ASAH1$^{Low}$ (gray) and ASAH1$^{High}$ (pink) ERMM and LRMM patients treated with proteasome inhibitor-based regimens and non-proteasome inhibitor-based regimens. Inset indicates median survival in days. Kaplan-Meier plots of duration of response (DoR; left), progression free survival (PFS; center) and overall survival (OS; right) of ASAH1$^{Low}$ (gray) and ASAH1$^{High}$ (pink) MM patients in CoMMpass IA16. Inset indicates median survival in days. NR = median survival not reached.

**f.** Bar chart of normalized ASAH1 protein abundance (ASAH1/actin) in PI resistant MM cells (PSR, V10-R, B25, C300R) relative to their respective PI-sensitive counterparts (U266, ANBL-6, 8226, 5TGM1). Values are mean ± SD of three independent experiments.

**Supplementary Figures and Legends**

Statistical significance was derived by Log-rank (Mantel-Cox) test (**b, e, f**) and ordinary one-way ANOVA with Dunnett's multiple comparisons test (**c, d, g**). p values of <0.05, <0.01, <0.001 and <0.0001 are represented by *, **, *** and **** respectively. Lines indicate statistical comparisons.

**Supplementary Figures and Legends**

Supp Figure 3

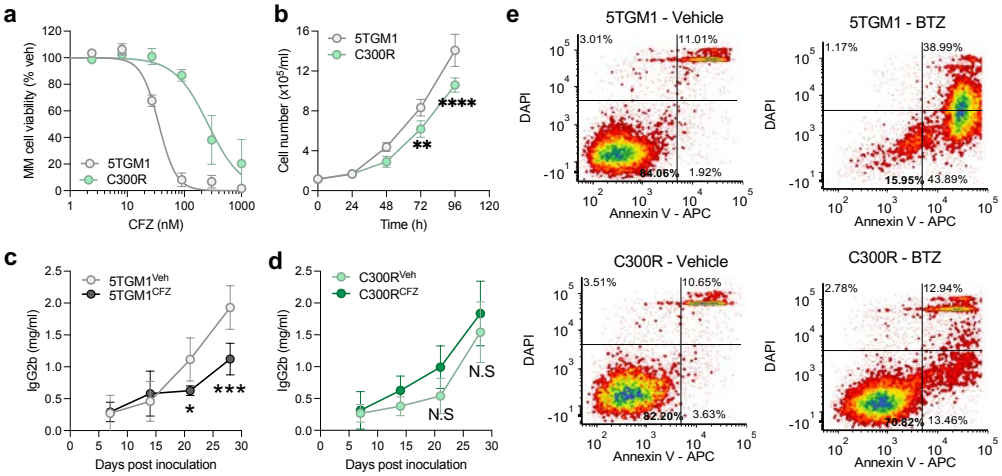


**Supplementary Figure 3. Characterization of proteasome inhibitor resistant C300R cells.**

**a.** Dose-response of parental 5TGM1 (gray) and derived PI-resistant C300R (green) myeloma cell lines with carfilzomib (CFZ) after 24 hours as assessed by MTS assay.

**b.** Growth of 5TGM1 and C300R *in vitro* over 96 hours.

**c.** Growth and response to twice-weekly carfilzomib (2 mg/kg i.v., consecutive days) or vehicle of parental 5TGM1 in C57Bl6/KalRwrij mice (n=5/group) as measured by serum IgG2b levels.

**d.** Growth and response to twice-weekly carfilzomib (2 mg/kg i.v., consecutive days) or vehicle of PI-resistant C300R in C57Bl6/KalRwrij mice (n=5/group) as measured by serum IgG2b levels.

**e.** Density plots showing levels of apoptosis (Annexin-V/DAPI) of 5TGM1 (top row) and C300R (bottom row) treated with vehicle (0.1% DMSO; left) or 10nM BTZ (right) for 24 hours.

**Supplementary Figures and Legends**

Statistical significance was derived by Ordinary one-way ANOVA with Dunnett's multiple comparisons test (**b**, **c, d**). p values of <0.05, <0.01, <0.001 and <0.0001 are represented by *, **, *** and **** respectively.

**Supplementary Figures and Legends**

Supp Figure 4

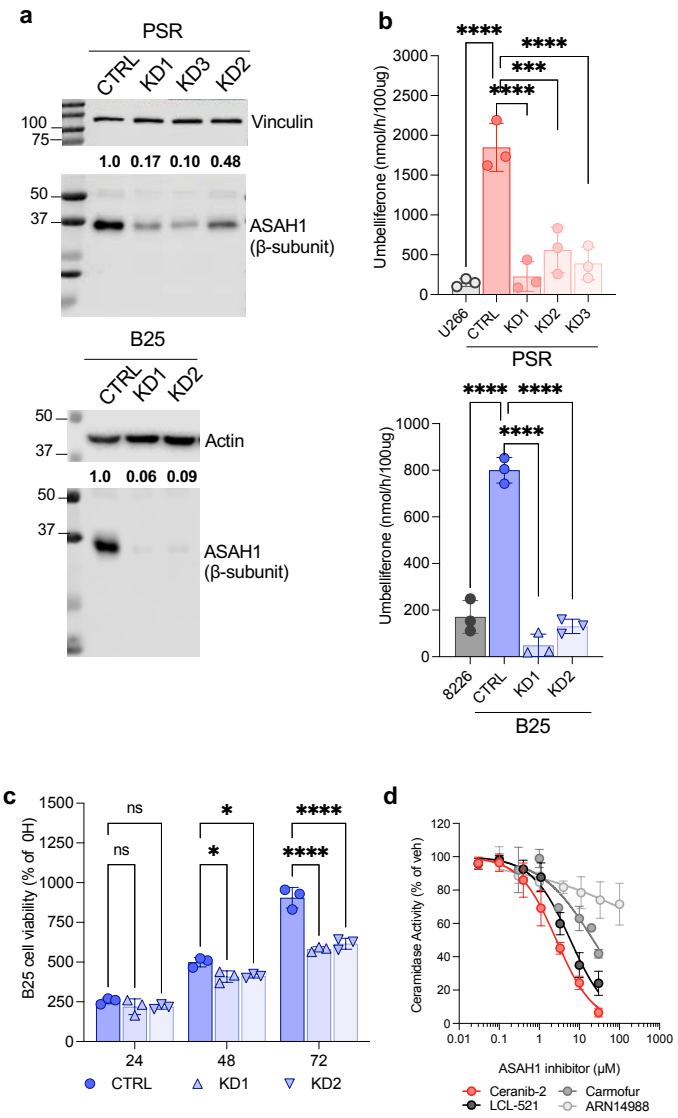


**Supplementary Figure 4. Inhibition of ASAH1 reduces ASAH1 activity and cell viability in relapsed/refractory multiple myeloma cell lines.**

**a.** Representative Immunoblots of ASAH1 and vinculin expression in PSR (top blot) nontargeting shRNA (CTRL) and ASAH1 shRNA knockdown cells (KD1-3). Emboldened values represent the normalized ASAH1 (ASAH1/vinculin) relative to the

non-targeting control MM cells. Representative Immunoblot of ASAH1 and actin expression in B25 (bottom blot) nontargeting shRNA (CTRL) and ASAH1 shRNA knockdown cells (KD1-2). Emboldened values represent the normalized ASAH1 (ASAH1/Actin) relative to the non-targeting control B25 cells.

**b.** Bar chart of ASAH1 activity as assayed by umbelliferone release from RBM14-C12 in PI sensitive U266 and PI resistant PSR (top) and PI sensitive 8226 and PI resistant B25 (bottom) MM cells with non-targeting shRNA (CTRL) or ASAH1 knockdown (KD1-3).

**c.** Bar chart of growth of control (CTRL) and ASAH1 knockdown (KD1/2) B25 MM cells as assessed by MTS at indicated time points.

**d.** Dose-response of ASAH1 enzymatic activity in PSR cells after 3 hours incubation in ASAH1 inhibitors at indicated concentrations.

Statistical significance was derived by Ordinary one-way ANOVA with Dunnett's multiple comparisons test (**b**, **c**). p values of <0.05, <0.001 and <0.0001 are represented by *, *** and **** respectively.

**Supplementary Figures and Legends**

Supp Figure 5

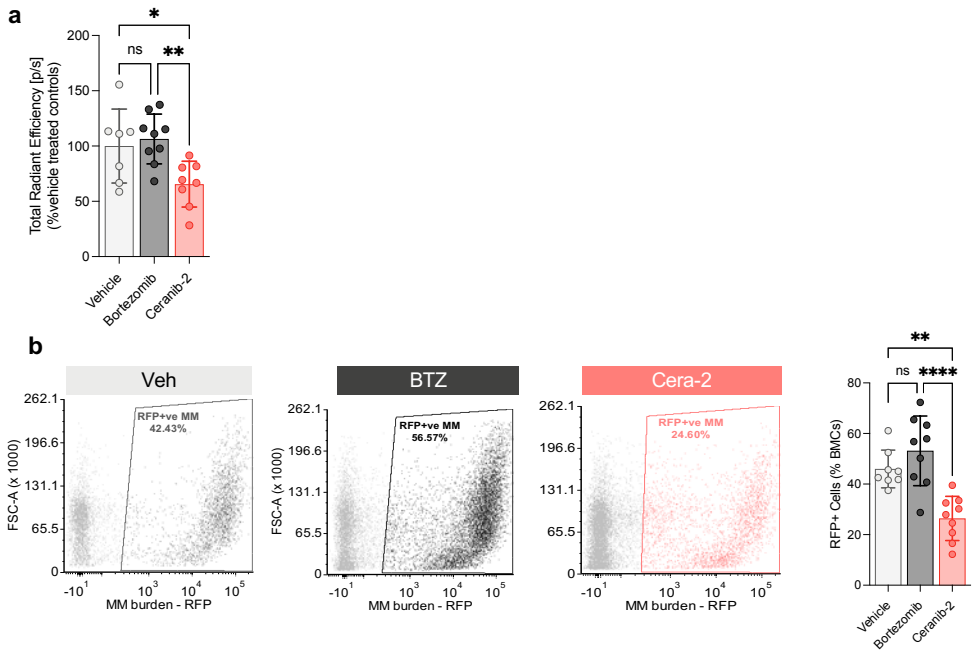


**Supplementary Figure 5. Treatment of relapsed/refractory multiple myeloma-bearing mice with ceranib-2 reduces tumor burden and suppresses osteolytic bone disease in mice.**

**a.** Bar chart of total radiant efficiency of mice in treated Cera-2 (n=8), BTZ (n=9), or vehicle (n=7) at the final time point in study including all mice normalized to the mean of the vehicle treated mice

**b.** Representative scatter plots of RFP+ Myeloma cells in bone marrow of mice in vehicle, bortezomib and ceranib-2 treated groups at end point (left). Quantification of the number of RFP+ MM cells as a percentage of live cells in the bones of mice treated with vehicle (n=7), bortezomib (n=9) or ceranib-2 (n=8) at end point.

**Supplementary Figures and Legends**

Statistical significance was derived by Ordinary one-way ANOVA with Dunnett's multiple comparisons test (**a**, **b**). p values of <0.05, <0.01 and <0.0001 are represented by *, ** and **** respectively. N.S = not significant.

**Supplementary Figures and Legends**

Supp Figure 6

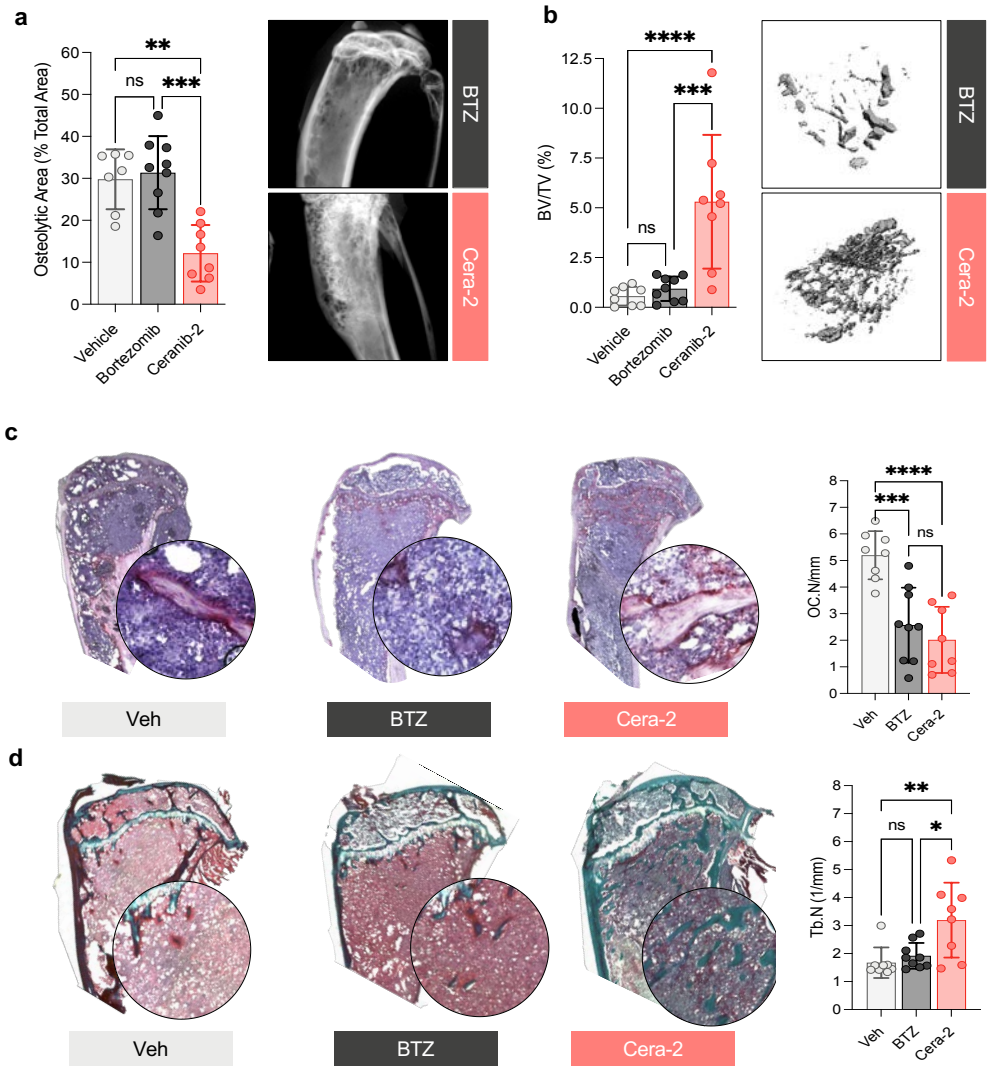


**Supplementary Figure 6. Treatment of relapsed/refractory multiple myeloma-bearing mice with ceranib-2 suppresses osteolytic bone disease in mice**

a. Bar chart quantification (left) of osteolytic area as a percentage of total bone area in tibia of mice treated with vehicle (n=7), ceranib-2 (n=8), or bortezomib (n=9) at

**Supplementary Figures and Legends**

endpoint. Representative x-ray images of bortezomib and ceranib-2 treated mice (right).

b. Bar chart (left) of trabecular bone volume as a percentage of tissue volume in tibia of mice treated with vehicle (n=7), ceranib-2 (n=8), or bortezomib (n=9) at endpoint. Representative μCT images (right) of osteolysis in bortezomib and ceranib-2 treated mice.

**c.** Representative micrographs (4X magnification; left) of TRAcP stained tibiae from mice in vehicle (n=7), ceranib-2 (n=8), or bortezomib (n=9) treated groups at end point. Inset = 20X. Bar chart (right) of osteoclast numbers per mm of bone surface in the trabecular of tibiae from mice in vehicle (n=7), ceranib-2 (n=8), or bortezomib (n=9) treated groups at end point.

**d.** Representative micrographs (4X magnification; left) of trichrome stained tibiae in vehicle, bortezomib and ceranib-2 treated groups at end point. Inset = 20X. Bar chart (right) of trabecular number in tibiae of mice in vehicle (n=7), ceranib-2 (n=8), or bortezomib (n=9) treated groups at end point as measured by microCT.

Statistical significance was derived by Ordinary one-way ANOVA with Dunnett's multiple comparisons test (**a**, **b**). p values of <0.05, <0.01, p<0.001 and <0.0001 are represented by *, **, *** and **** respectively. N.S = not significant. Lines indicate the statistical comparison.

**Supplementary Figures and Legends**

Supp Figure 7

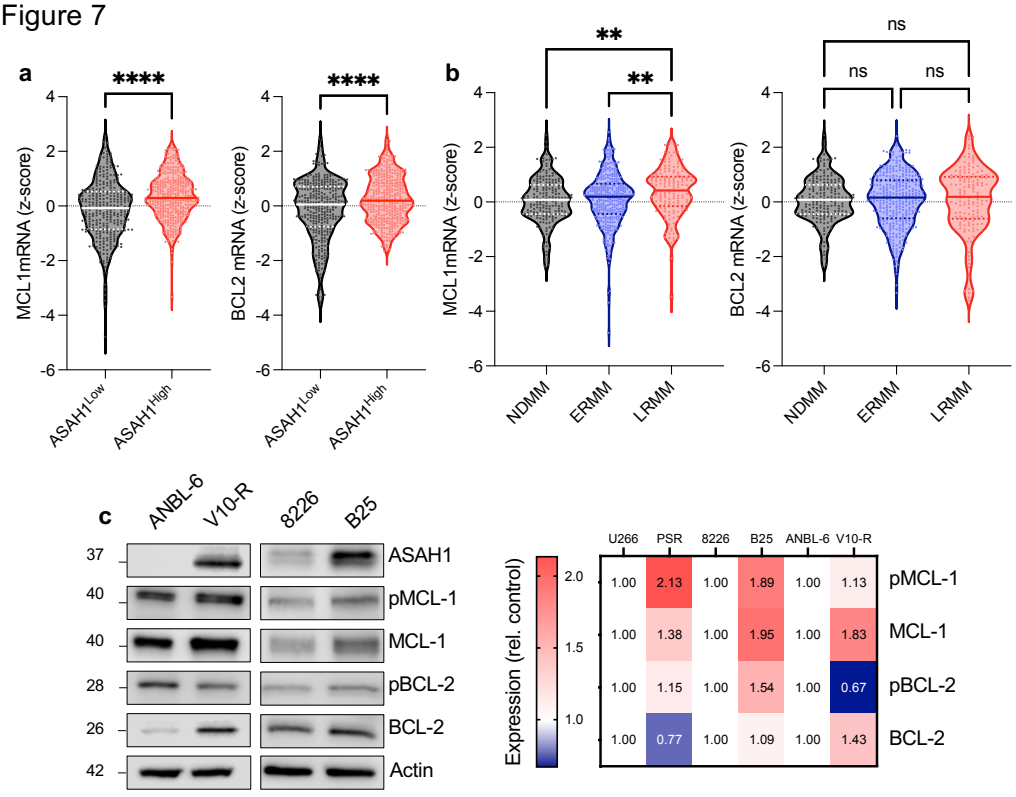


**Supplementary Figure 7. ASAH1 is associated with MCL-1 and BCL-2 levels in relapsed/refractory multiple myeloma.**

**a.** Violin plot of MCL1 mRNA expression (left) in ASAH1$^{Low}$ (gray; n=323) ASAH1$^{High}$ (pink n=349) Pentecost Myeloma Research Center (PMRC) multiple myeloma (MM) patients. Violin plot BCL2 mRNA expression (right) in ASAH1$^{Low}$ (gray; n=321) ASAH1$^{High}$ (pink n=351).

**b.** Violin plot of MCL1 and BCL2 mRNA expression (Z-score) in newly diagnosed multiple myeloma (NDMM, n=187), early relapse multiple myeloma (ERMM, n=303) and late relapse multiple myeloma (LRMM, n=182) PMRC patients.

**Supplementary Figures and Legends**

**c.** Immunoblot of ASAH1, pMCL-1 (T163), total MCL-1, p-BCL-2 (S70), and total BCL-2 expression in PI-sensitive (ANBL6, 8226) and PI-resistant (V10-R, B25) MM cells. Heatmap showing the mean house-keeping protein normalized expression of pMCL-1 (T163), total MCL-1, p-BCL-2 (S70), and total BCL-2 expression relative to PI-sensitive controls in PI-sensitive (U266, ANBL6, 8226) and PI-resistant (PSR, V10-R, B25) MM cells. Values are mean ± SD of at least two independent experiments. Statistical significance was derived by unpaired t -test (**a**) or ordinary one-way ANOVA with Dunnett's multiple comparisons test (**b**). p values of <0.01 and <0.0001 are represented by ** and **** respectively. N.S = not significant. Lines indicate the statistical comparison.

**Supplementary Figures and Legends**

Supp Figure 8

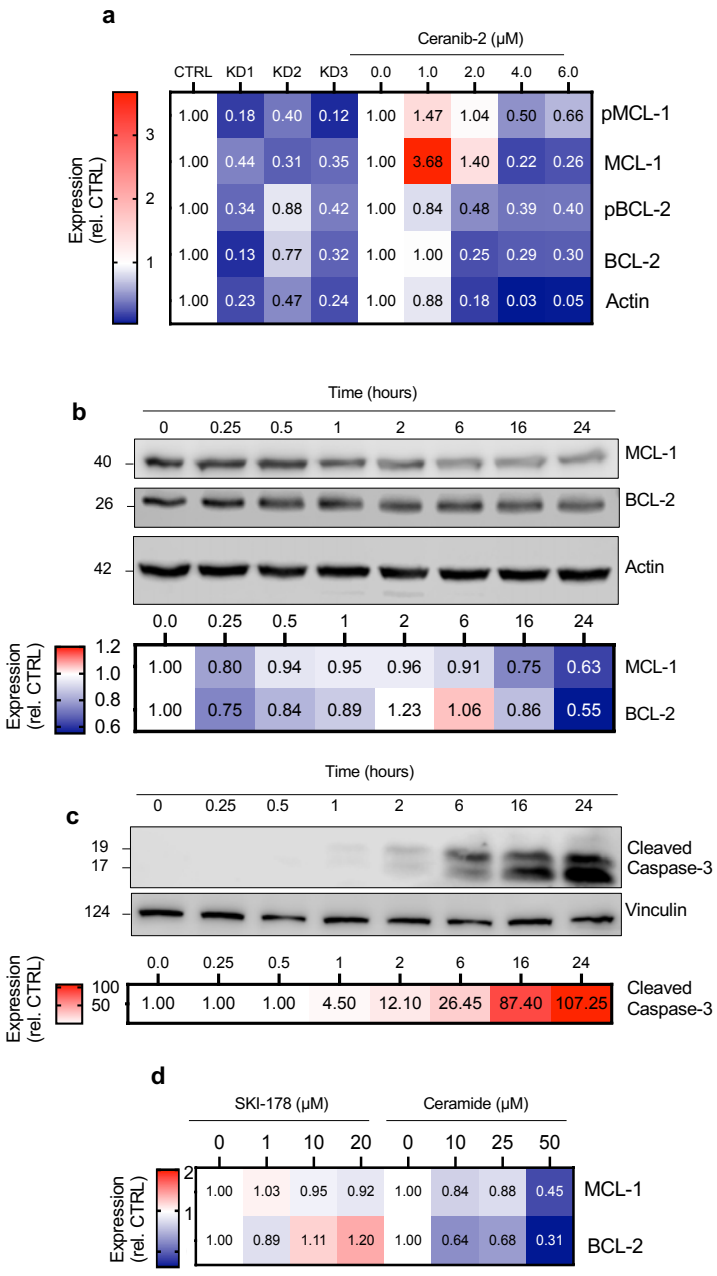


**Supplementary Figure 8. ASAH1 is associated with MCL-1 and BCL-2 levels in relapsed/refractory multiple myeloma.**

**Supplementary Figures and Legends**

**a.** Heatmap showing the mean normalized expression of ASAH1, pMCL-1 (T163), total MCL-1, p-BCL-2 (S70), and total BCL-2 expression in control (CTRL) or ASAH1 knockdown (KD1-3) PSR multiple myeloma (MM) cells or PSR MM cells treated with 2 μM ceranib-2 for indicated number of hours, relative to either CTRL or vehicle treated PSR cells. Values are mean of two independent experiments.

**b.** Immunoblot (top) of total MCL-1 and total BCL-2 expression in PI-resistant V10-R MM cells treated with 5 μM ceranib-2 and 1 ng/mL IL-6 at indicated times post treatment. Heatmap (bottom) showing the mean normalized expression of total MCL-1 and total BCL-2 expression in V10-R cells in response to 5 μM ceranib-2. Values are mean of two independent experiments

**c.** Immunoblot (top) of cleaved caspase-3 expression in PI-resistant V10-R MM cells treated with 5 μM ceranib-2 and 1 ng/mL IL-6 at indicated times post treatment. Heatmap (bottom) showing the mean normalized expression of cleaved caspase-3 expression in V10-R cells in response to 5 μM ceranib-2. Values are mean of two independent experiments

**d.** Heatmap showing the mean normalized expression of total MCL-1 and total BCL-2 expression in PSR MM cells treated with indicated concentrations of sphingosine kinase inhibitor SKI-178 or ceramide C6 for 4 hours. Values are mean of two independent experiments

**Supplementary Figures and Legends**

Supp Figure 9

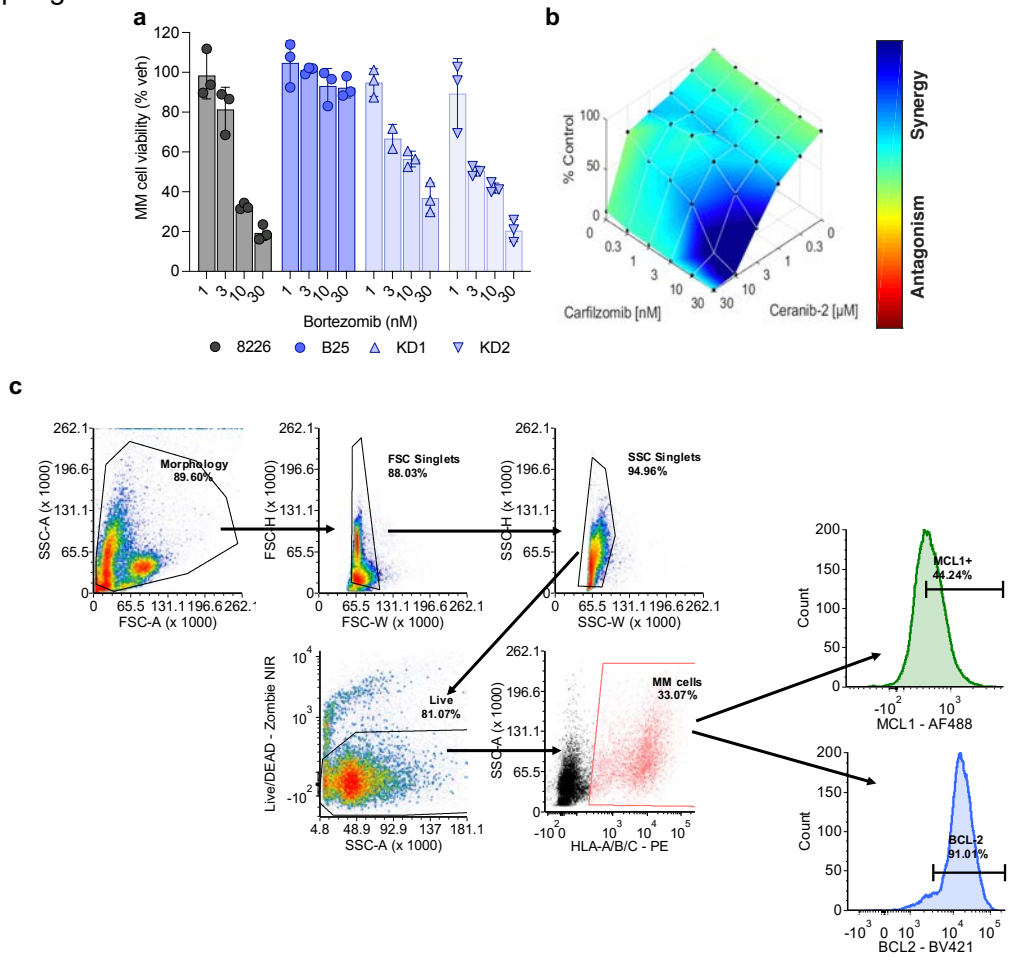


**Supplementary Figure 9. Inhibition of ASAH1 restores PI-sensitivity in relapsed/refractory multiple myeloma cell lines.**

**a.** Bar chart showing the effect of indicated concentrations of BTZ on 8226, CTRL (B25) and ASAH1 KD (KD1/2) B25 cell viability after 24 hours as assessed by MTS assay.

**b.** LOEWE synergy plot showing the effect of indicated concentrations of ceranib-2 and carfilzomib as single agents and in combination on C300R murine MM cells after 24 hours as assessed by MTS assay.

**Supplementary Figures and Legends**

**c.** Flow cytometry gating strategy for identification of HLA A/B/C+ MCL-1+ and BCL2+ MM cells in the bone marrow of mice *ex vivo* studies in Figure **4**.

**Supplementary Figures and Legends**

Supp Figure 10

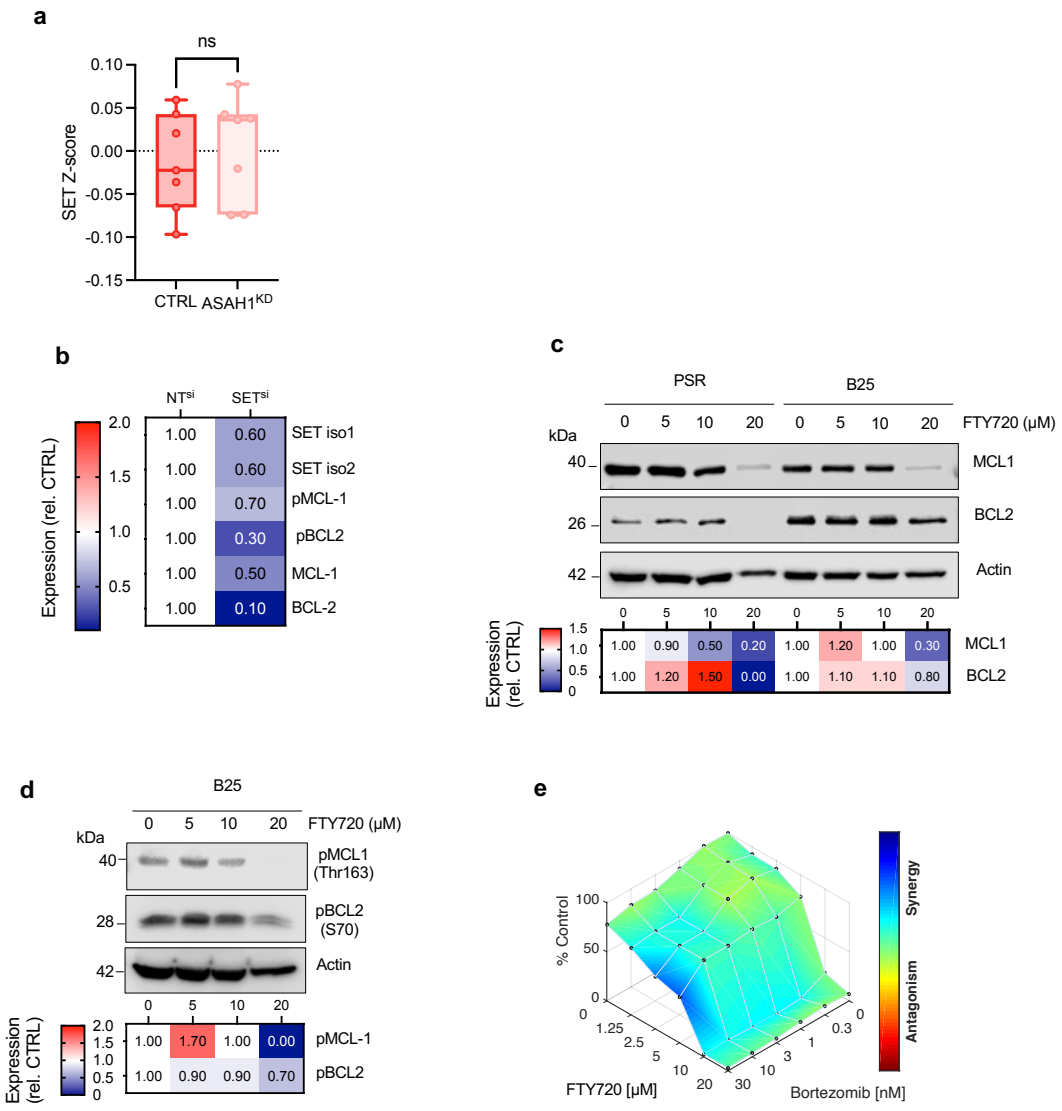


**Supplementary Figure 10. SET is associated with relapse and resistance to proteasome inhibitors in relapsed/refractory multiple myeloma.**

**a.** Box and whisker plot of SET expression (normalized Z-score) in CTRL and ASAH1 KD PI resistant multiple myeloma (MM) cells quantitated by LC-MS/MS proteomics. Each dot represents a biological replicate (n=7/group).

**Supplementary Figures and Legends**

**b.** Heatmap quantification of protein expression of SET isoforms 1 and 2, total and phosphorylated MCL-1 and BCL-2 48 hours following transfection of PSR cells with non-targeting siRNA (NTsi) or SET-targeting siRNA (SETsi) normalized to housekeeping protein relative to non-targeting siRNA (NTsi) controls. Values are mean of 3 independent experiments.

**c.** Immunoblot (top) of MCL1, BCL2 and actin following treatment with indicated concentration of FTY-720 (4 hours) in PI-resistant MM cell lysates. Heatmap quantification (bottom) of protein expression normalized to housekeeping protein relative to vehicle treated controls. Values are mean of 3 independent experiments.

**d.** Immunoblot (top) of phosphorylated MCL1 (Thr163), phosphorylated BCL2 (S70) and actin following treatment with indicated concentration of FTY-720 (4 hours) in PI-resistant MM cell lysates. Heatmap quantification (bottom) of protein expression normalized to housekeeping protein relative to vehicle treated controls.

**e.** LOEWE synergy plot of the viability of PSR MM cells 24 hours after treatment with indicated concentrations of FTY-720 and BTZ.

Statistical significance was derived by unpaired t -test (**a**). N.S = not significant.

**Supplementary Figures and Legends**

Supp Figure 11

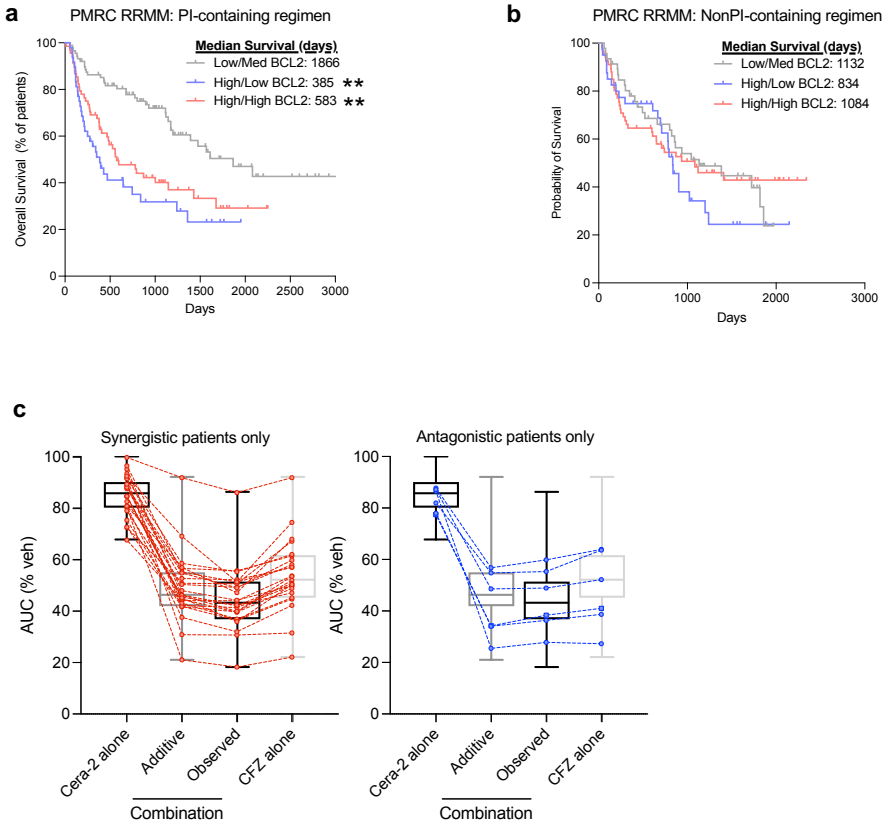


**Supplementary Figure 11. Ceranib-2 synergizes with carfilzomib in most *ex vivo* multiple myeloma patient samples.**

**a.** Kaplan-Meier plot of overall survival of relapsed/refractory multiple myeloma (RRMM) patients treated with PI-containing regimen in each cluster. Low/Med BCL-2 (gray), High/Low BCL-2 (blue), High/High BCL-2 (pink). Inset indicates median survival in days.

**b.** Kaplan-Meier plot of overall survival of relapsed/refractory multiple myeloma (RRMM) patients treated with NonPI-containing regimen in each cluster. Low/Med BCL-2 (gray), High/Low BCL-2 (blue), High/High BCL-2 (pink). Inset indicates median survival in days

**Supplementary Figures and Legends**

**c.** Box and whisker plot showing the median AUC of 30 patients' (1 smoldering multiple myeloma (SMOL), 1 plasma cell leukemia (PCL), 14 newly diagnosed multiple myeloma (NDMM) and 14 relapsed/refractory multiple myeloma (RRMM) patients' response *ex vivo* to single agent ceranib-2 (cera-2), carfilzomib (CFZ), or the combination – either additive or observed. Additive represents the expected value of combining two agents whereas observed indicates the actual response. The difference between additive and observed values is used to calculate either synergy or antagonism. Red dots and lines represent synergy (left plot, n=24) whereas blue lines and dots represents antagonism (right plot, n=6).

Statistical significance was derived by Log-rank (Mantel-Cox) test (**a, b**). p values of <0.01 are represented by ** and denote statistical difference to Low/Med BCL2 group.

**Supplementary Figures and Legends**

## References

1. Chen S, Dai Y, Pei XY, et al. CDK inhibitors upregulate BH3-only proteins to sensitize human myeloma cells to BH3 mimetic therapies. Cancer Res. 2012;72(16):4225-4237.
2. Chen S, Zhang Y, Zhou L, et al. A Bim-targeting strategy overcomes adaptive bortezomib resistance in myeloma through a novel link between autophagy and apoptosis. Blood, 2014:2687-2697.
3. Zhuang J, Shirazi F, Singh RK, et al. Ubiquitin-activating enzyme inhibition induces an unfolded protein response and overcomes drug resistance in myeloma. Blood. 2019;133(14):1572-1584.
4. Silva A, Jacobson T, Meads M, Distler A, Shain K. An Organotypic High Throughput System for Characterization of Drug Sensitivity of Primary Multiple Myeloma Cells. Jove-J Vis Exp. 2015;101):
5. Cox J, Mann M. MaxQuant enables high peptide identification rates, individualized p.p.b.-range mass accuracies and proteome-wide protein quantification. Nat Biotechnol. 2008;26(12):1367-1372.
6. Tyanova S, Temu T, Sinitcyn P, et al. The Perseus computational platform for comprehensive analysis of (prote)omics data. Nat Methods. 2016;13(9):731-740.
7. Yilmaz S, Ayati M, Schlatzer D, Cicek AE, Chance MR, Koyuturk M. Robust inference of kinase activity using functional networks. Nat Commun. 2021;12(1):1177.

## Supplementary Figures and Legends